Nonlinear Dyn
https://doi.org/10.1007/s11071-025-11742-8

RESEARCH

A mathematical approach to spark ignition process in premixed flame systems: modeling and analysis

Chunkan Yu · **Felipe Minuzzi**

Received: 4 February 2025 / Revised: 12 July 2025 / Accepted: 22 August 2025

Abstract This study enhances the classic perfectly stirred reactor model by introducing an additional energy source to effectively model the spark ignition process within a laminar premixed flame in a counterflow configuration. A non-dimensional governing ordinary differential equation (ODE) system is developed to describe the behavior of both temperature and fuel concentration under these conditions. An in-depth mathematical analysis is performed to find out the stability of steady-state solutions within the dynamic system, using the large activation energy asymptotic limit as a key analytical approach. Solutions corresponding to stable regimes are derived analytically, which is characterized by negative eigenvalues. This analytical framework is further extended through the direct integration of the non-dimensional ODE system, allowing an investigation on how critical parameters – including the Damköhler number, spark duration time, and the heat released during chemical reactions – affect the ignition process. Particular attention is given to the calculation of the minimum ignition energy , providing valuable insights into optimizing ignition strategies in practical applications.

C. Yu (✉)
Institute of Technical Thermodynamics, Karlsruhe Institute of Technology, Engelbert-Arnold-Straße 4, 76131 Karlsruhe, Baden-Württemberg, Germany
e-mail: chunkan.yu@kit.edu

F. Minuzzi
Institute of Mathematics and Statistics, Federal University of Rio Grande Do Sul, Porto Alegre, 90060-040 RS, Brazil

Keywords PSR · Spark ignition · Dynamic system · Non-dimensionalization · Minimum ignition energy (MIE)

1 Introduction

There have been numerous studies aimed at clarifying the spark ignition process of premixed combustible gas mixtures in various configurations, as understanding this process is crucial for optimizing combustion efficiency and safety in engines and industrial applications. In [1], the authors model and numerically investigate the effect of the initial pressure wave generated by the spark on the minimum ignition energy (MIE), which plays a critical role in determining the success or failure of ignition in various operational conditions. Their study highlights the importance of accounting for pressure wave dynamics in accurately predicting MIE in practical combustion systems. Further investigations such as [2,3] focus on calculating MIE for a range of parameters, including mixture compositions, pressures, radii of external energy sources, and ignition times. These studies provide insights into how these factors influence the energy threshold required to ignite premixed gases, offering valuable data for both cylindrical and spherical geometries.

In addition to numerical simulations grounded in detailed chemical kinetics, theoretical analyses have been developed to generalize the behavior observed during the spark ignition process. For instance, [4]

Published online: 08 September 2025

presents a theoretical study on the dynamic development of outwardly propagating spherical flames initiated by external energy deposition. This study discussed the effects of key parameters, such as the Lewis number and Karlovitz number, on flame kernel initiation, providing a deeper understanding of the flame propagation and stability during the early stages of ignition. [5] offers a theoretical framework for analyzing spark ignition in premixed flames, focusing on two-step reaction mechanisms, namely chain-branching and recombination reactions. This study examines how these reactions interact during the ignition process, providing a more comprehensive understanding of the chemical kinetics involved. Such analyses are essential for understanding the interaction between chemical kinetics and ignition process in a generic way. Additionally, a comprehensive review on spark ignition in laminar premixed flames can be found in [6], which focuses on theoretical developments and summarizes various analytical models and asymptotic analyses. This review focused on existing knowledge on the subject and provides an overview of the progress made in understanding the ignition mechanisms from a theoretical perspective, highlighting key challenges and opportunities for future research.

Recently, the relatively new configuration of spark ignition of laminar premixed flame in counterflow [7,8] has been proposed and numerically investigated. This configuration provides the possibility to investigate the spark ignition process under a constant flame strain rate, an indicator used to describe the flow velocity and velocity gradient along the flame surface. This can largely simplify the complexity involved in spherical flames, where during the spark ignition process, the flame strain rate changes rapidly during flame propagation [9,10]. In [7,8], it was reported that the MIE increases with larger flow velocity, as more gas mixture passes through the energy source region. Additionally, at short spark duration times, the MIE shows only minor changes. While previous studies have investigated spark ignition in strained laminar premixed flames using detailed numerical simulations for specific fuel-air mixtures (e.g., methane/hydrogen/air [8] and ammonia/hydrogen/air [7]), these works did not provide a simplified theoretical framework that captures the general influence of flow conditions such as strain rate on ignition behavior. In particular, the underlying mechanism by which flow-driven residence time interacts with chemical timescales to govern ignition has not been analytically clarified. To address this gap, the present study develops a reduced theoretical model based on the classical Perfectly Stirred Reactor (PSR) framework, augmented with the energy source to represent spark input. This approach enables direct comparison between flow-controlled residence time and chemical reaction time, providing generalized insights into the critical conditions for ignition across different mixtures and operating parameters.

The PSR model has been selected as the simple model, since it has long been recognized as a powerful tool for capturing key combustion phenomena in a highly simplified yet physically meaningful framework. It has been extensively applied to study ignition and extinction limits, flame stabilization, nonlinear oscillations, and bifurcation behavior under various conditions. Representative examples include the investigation of complex combustion dynamics using reduced chemical models [11], bifurcation analysis of limit flames in DME/air systems [12], near ignition/extinction regimes [?], and the coupling of velocity nonuniformity with wall heat loss in supersonic mixing layer flames [13]. These applications show the applicability of the PSR framework in exploring a wide range of combustion phenomena. Therefore, this model is further extended by incorporating a localized energy source in the present work, allowing us to enable the analytical tractability of the PSR model while capturing the essential physics of the ignition process.

The present paper is organized as follows: Sect. 2 introduces the governing equations for temperature and fuel mass fraction in their non-dimensional form, derived by introducing various dimensionless variables relevant to the spark ignition process. In Sect. 3, the stability of the steady-state solutions is examined through an eigenvalue analysis of the dynamic system. Section 4 explores the influence of key dimensionless variables, such as the Damköhler number, heat release, and spark ignition parameters, on the minimum ignition energy and ignition behavior by directly integrating the non-dimensional ODE system. Finally, Sect. 5 provides a summary of the conclusions drawn from the study.

2 Mathematical modeling of perfectly stirred reactor (PSR)

Figure 1 (left) illustrates the spark ignition process in a laminar premixed flame under a counterflow configura-

tion, as investigated in [7,8]. In this setup, two opposing streams of premixed unburnt fuel-oxidizer mixture are directed toward each other. A spark igniter is placed at the stagnation plane, where energy is deposited within a specified spark width over a certain spark duration, thereby heating the gas mixture in that region. The counterflow setup allows precise control of the strain rate, which refers to the rate at which the two opposing streams stretch the flame front due to the velocity gradient along it [14,15]. A higher strain rate corresponds to a higher flow velocity of the unburnt gas mixture. According to previous studies [7,8], the required energy for successful ignition increases with increasing strain rate, i.e., with increasing flow velocity. While the counterflow configuration is well-suited for capturing the relationship between ignition energy and flow field, as well as the influence of physical and chemical time scales on ignition behavior, direct analytical treatment of this configuration is complex. This is due to the presence of unsteady terms (time derivatives), convective transport (first-order spatial derivatives), and molecular transport processes such as species diffusion and heat conduction (second-order spatial derivatives). These effects result in a transient system of partial differential equations (PDEs), which are challenging to solve analytically or even analyze systematically. Therefore, in this work, we focus on the region between two spark igniters, as indicated by the green-shaded area in Figure 1.

Within this region, the gas mixture is heated by the deposited ignition energy. During the entire process, fresh cold unburnt gas continuously enters the region and mixes with the heated mixture, while the resulting mixture also leaves the region. Depending on the amount of ignition energy, the outgoing mixture may either successfully ignite or fail to ignite due to excessive dilution by the incoming cold reactants. Additionally, the flow velocity determines the residence time of the heated mixture in the ignition region. At higher flow velocities (corresponding to higher flame strain rates), the residence time becomes shorter, reducing the opportunity for successful ignition.

Based on these observations, the classical Perfectly Stirred Reactor (PSR) model [16] can be adopted with additional consideration of an external energy source, as illustrated in Figure 1 (right). The PSR framework effectively captures the key features of the ignition region discussed above, including energy deposition, mixing with incoming reactants, and residence time controlled ignition behavior. Initially, unburnt premixed gas mixture fills the reactor, and spark ignition energy is provided to heat the entire gas mixture inside. During and after the spark process, fresh unburnt gas mixture entering the reactor cools the heated gas mixture in a perfectly mixed manner, which then leaves the reactor. The steady state of the PSR model provides information about whether sufficient energy was initially provided to sustain further chemical reactions. If the gas mixture leaving the reactor is the same as the unburnt gas mixture at steady state, the system has not been successfully ignited. If the gas mixture leaving the reactor is at a high temperature and has mostly converted to products at steady state, the system has been successfully ignited.

It should be additional mentioned that although diffusion processes are important in realistic ignition phenomena, the present model accounts for such effects indirectly through the residence time. Specifically, shorter residence times correspond to higher flow velocities, which reduce the time available for thermal and species diffusion to establish significant gradients within the ignition region. Therefore, the model captures the essential balance between chemical timescales and flow-induced mixing governed by diffusion in physical systems.

2.1 Mathematical modeling

2.1.1 Mathematical formulation

The Perfectly Stirred Reactor (PSR) model considered here involves several futher assumption, as follows:

- there is no heat loss from the reactor to the surrounding.
- all physical properties such as density $\widetilde{\rho}$ and heat capacity $\widetilde{c}_p$ are constant values, which are not dependent on the temperature.
- one step global reaction F(uel)→P(roduct) is considered and the reaction rate is governed by the Arrhenius law with reactor order 1. Note that while this one-step global mechanism captures the overall reaction trends, it neglects detailed chemistry involving intermediate species. Thus, the predicted predicted minimum ignition energy (MIE) in the present work should be regarded as qualitative. Quantitatively reliable predictions would require a detailed chemical kinetic mechanism (c.f. [7,8]).

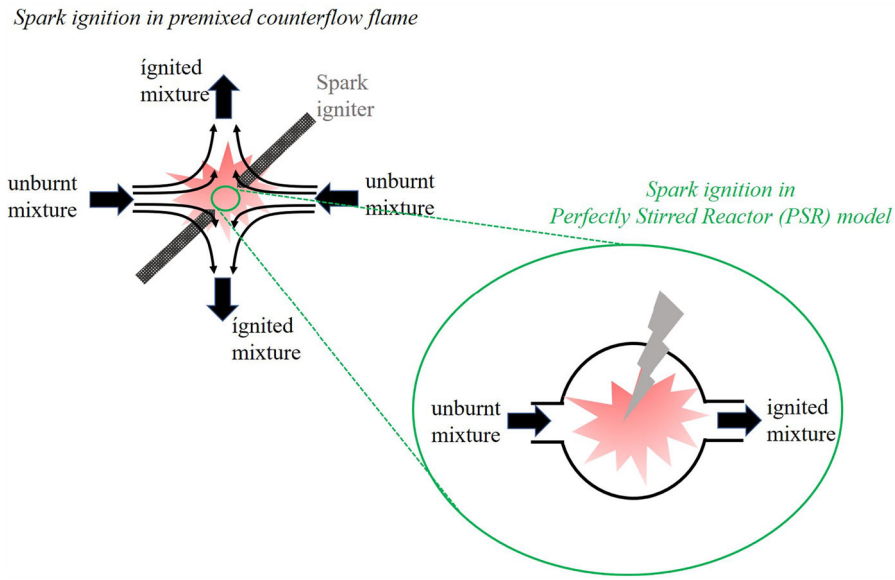

Fig. 1 Schematic illustration for modeled spark ignition process in Perfectly Stirred Reactor (PSR)

- the volumetric spark ignition energy $\widetilde{E}_s$ is used to heat up the whole gas mixture inside the PSR within a certain spark deposited time $\widetilde{\tau}_s$, and its power $\dot{\widetilde{E}}_s = \widetilde{E}_s/\widetilde{\tau}_s$ is constant over time. Note that in this study the spark is treated as a volumetric energy source within a PSR that represents the small ignition region (green zone in Fig. 1). The perfect-mixing assumption lets us express the energy balance per unit volume, even though an actual spark is spatially and temporally localized.
- Given the perfectly stirred reactor assumption (implying infinitely fast mixing) and the fact that spark ignition primarily involves fuel heating before reactions begin [7,17], the use of a single mixing time scale does not affect the qualitative conclusions.

Based on these assumptions, the following conservation equations for energy in terms of temperature $\widetilde{T}$ and volumetric fuel concentration $\widetilde{c}_F$ can be written as:

$$\widetilde{\rho}\widetilde{c}_p \frac{\mathrm{d}\widetilde{T}}{\mathrm{d}\widetilde{t}} = -\widetilde{\rho}\widetilde{c}_p \frac{\widetilde{T} - \widetilde{T}_{\mathrm{in}}}{\widetilde{\tau}_R} + \widetilde{Q}\dot{\widetilde{\omega}}_F + \dot{\widetilde{E}}_s \tag{1}$$

$$\frac{\mathrm{d}\widetilde{c}_F}{\mathrm{d}\widetilde{t}} = -\frac{\widetilde{c}_F - \widetilde{c}_{F,\mathrm{in}}}{\widetilde{\tau}_R} - \dot{\widetilde{\omega}}_F. \tag{2}$$

In these equations, $\widetilde{T}$ is the temperature inside the reactor, $\widetilde{c}_F$ the volumetric fuel concentration, and $\widetilde{\tau}_R$ the residence time. $\widetilde{T}_{\mathrm{in}}$ and $\widetilde{c}_{F,\mathrm{in}}$ are the temperature and volumetric fuel concentration of the incoming gas mixtures entering the reactor. $\widetilde{Q}$ denotes the heat release of the reaction, $\dot{\widetilde{\omega}}_F$ the consumption rate of fuel due to chemical reaction, which is expressed as:

$$\dot{\widetilde{\omega}}_F = \widetilde{A}\widetilde{c}_F \exp\left(-\frac{\widetilde{E}_a}{\widetilde{R}\widetilde{T}}\right), \tag{3}$$

where $\widetilde{A}$ is the pre-exponential factor, $\widetilde{E}_a$ the activation energy and $\widetilde{R}$ the universal gas constant.

For power of spark ignition energy, it follows the case conditions that i) $\dot{\widetilde{E}}_s = \widetilde{E}_s/\widetilde{\tau}_s$ for $\widetilde{t} \le \widetilde{\tau}_s$; and ii) $\dot{\widetilde{E}}_s = 0$ for $\widetilde{t} > \widetilde{\tau}_s$.

2.1.2 Non-dimensionalization

The above mentioned governing equation can be written in non-dimensional formulation by introducing several dimensionless variables listed in Tab.1.

$$\frac{\mathrm{d}\theta}{\mathrm{d}t} = -\theta + BDa(1-c_F)\exp\left(\frac{\theta}{1+\theta/\beta}\right) + \dot{e}_s,$$

$$\text{with } \dot{e}_s = \begin{cases} \frac{e_s}{\tau_s} & (t \le \tau_s) \\ 0 & (t > \tau_s) \end{cases} \tag{4}$$

$$\frac{\mathrm{d}c_F}{\mathrm{d}t} = -c_F + Da(1-c_F)\exp\left(\frac{\theta}{1+\theta/\beta}\right), \tag{5}$$

with the initial condition

$$\theta(t=0) = 0, \quad \text{and} \quad c_F(t=0) = 0. \tag{6}$$

For $c_F = 0$, the gas mixture consists only of fuel, while for $c_F = 1$, the fuel is fully converted into product. For $0 < c_F < 1$, the gas mixture consists of both fuel and product. At steady state, if the mixture leaves the reactor with $c_F \approx 0$, the system has not been successfully

Table 1 Dimensionless variables

Description	Dimensionless variable
Dimensionless activation energy	$\beta = \frac{\widetilde{E}_a}{\widetilde{R}\widetilde{T}_{\text{in}}}$
Dimensionless heat release	$B = \frac{\widetilde{Q}\beta}{\widetilde{\rho}\widetilde{c}_p\widetilde{T}_{\text{in}}}\widetilde{c}_{F,\text{in}}$
Dimensionless time	$t = \frac{\widetilde{t}}{\widetilde{\tau}_R}$
dimensionless fuel conversion	$c_F = \frac{\widetilde{c}_{F,\text{in}} - \widetilde{c}_F}{\widetilde{c}_{F,\text{in}}}$
Dimensionless temperature	$\theta = \frac{\beta(\widetilde{T} - \widetilde{T}_{\text{in}})}{\widetilde{T}_{\text{in}}}$
Damköhler number	$Da = \frac{\tau_R}{\tau_{\text{chem}}} = \frac{\widetilde{\tau}_R}{\left[\widetilde{A}\exp(-\beta)\right]^{-1}}$

ignited. If the mixture leaves the reactor with $c_F \approx 1$, then most of the fuel has been converted into product, indicating successful ignition. It should be noted that while the reaction rate is finite at $\theta = 0$, the dimensionless fuel conversion c_F inside the reactor is initially zero. Reaction only starts after the fuel enters the reactor. Therefore, nonzero rates at the inlet temperature reflect auto-ignition behavior, not pre-reaction outside the domain.

This dimensionless ODE system consists of three important dimensionless parameters: the dimensionless activation energy β, the dimensionless heat release B, and the Damköhler number Da. The dimensionless activation energy β is much larger than 1 for chemical reactions in combustible gas mixtures and is typically considered to be in the range of $30 \leq \beta \leq 50$ [18,19]. The dimensionless heat release B can range from small (indicating a weak exothermic reaction) to large (indicating a strong exothermic reaction). The third dimensionless parameter is the Damköhler number (Da), which is a critical parameter that describes the ratio of the flow time scale (in this case, the residence time) to the chemical reaction time scale. The proposed simplified PSR model is useful because flows with higher strain rates have higher convective mass transfer rates, which correspond to lower Da values. In experiments, regime with lower Da values can be achieved by either using diluted mixtures (longer chemical timescale) or imposing fast flow (shorter residence time). Although high-speed flows may involve turbulence, the present model focuses on a small, well-mixed ignition zone (c.f. Fig. 1) where residence time remains short.

A time integration of the above ODE system wills be performed using MATLAB throughout the whole work. To address potential stiffness in the system, the implicit solver ode15s was used.

2.2 Failed and successful spark ignition modes

Figure 2 shows the typical time development of dimensionless temperature and fuel concentration for a failed ignition (left) and a successful ignition (right). In both cases, the spark duration time is 0.1, as indicated by the vertical dashed lines. The only difference between the two cases is the provided spark ignition energy e_s. For a failed ignition with low spark ignition energy (here $e_s = 1$), the dimensionless fuel conversion at steady state is as low as 0.05, indicating that almost no fuel is converted into the product, and the corresponding dimensionless temperature remains well below 1. However, for a successful ignition with sufficiently high spark ignition energy (here $e_s = 4$), a sharp increase in fuel concentration is observed, reaching almost 1.0 at steady state, with the corresponding dimensionless temperature rising to around 8.

From this example, we observe that, for the same values of dimensionless variables, the dynamic system can reach different steady states depending on the provided spark ignition energy. This shows the system's sensitivity to input spark energy, where small changes in spark energy can lead to entirely different ignition modes. In the following, we will discuss some mathematical analysis of the dynamic system to better understand the underlying mechanisms governing these divergent behaviors.

3 *A-priori* mathematical analysis

As shown in the previous section, the system can have two different solutions. In this section, we will investigate some fundamental aspects of the dynamic system, including the stability of the steady-state solutions and how these steady states change with respect to the dimensionless variables. This analysis will focus on the mathematical properties of the system without focusing too much on the physical reasons behind these behaviors, which will be discussed in the next section.

For the steady-state (SS) condition ($\mathrm{d}\theta/\mathrm{d}t = 0$, $\mathrm{d}c_F/\mathrm{d}t = 0$, $e_s = 0$), the manifold for the steady-state

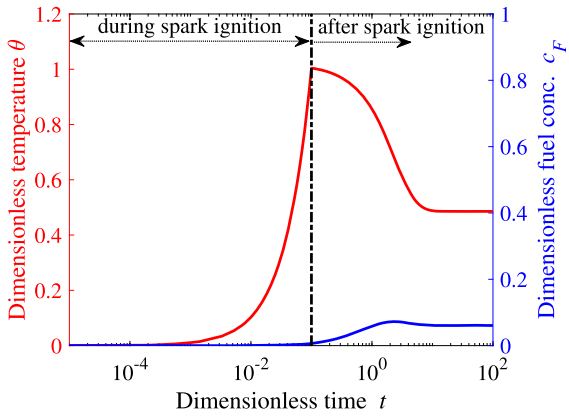

(a) Failed spark ignition: $e_s = 1$.

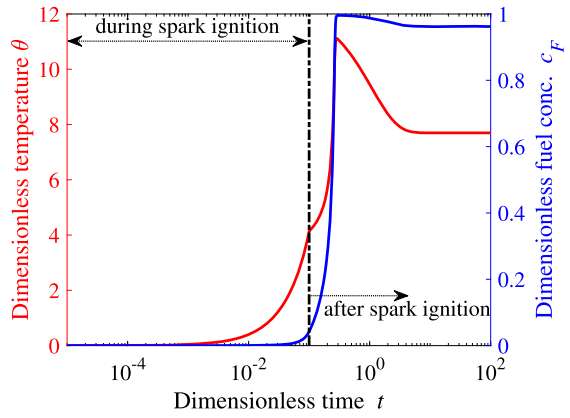

(b) Successful spark ignition: $e_s = 4$.

Fig. 2 Time-development of dimensionless temperature and fuel concentration for a failed ignition (left) and a successful ignition (right). Model parameter: $B = 8$, $\tau_s = 0.1$, $\beta = 40$, $Da^{-1} = 25$

solution is obtained as:

$$\theta^{\text{ss}} = B \cdot c_F^{\text{ss}}. \tag{7}$$

It can be observed that the steady-state solution is a linear function with a constant slope, where the slope is determined by the dimensionless heat release variable B. This indicates that the steady-state solution depends solely on the value of B.

As shown in Fig. 2, for successful ignition, the value of θ is typically around 10, while for unsuccessful ignition cases, it remains even much lower, often below 1. Given that β is in the range of 30-50 [18,19], the condition $\theta/\beta \ll 1$ is satisfied in all cases. Under this condition, the exponential term can be approximated as $\exp\left(\frac{\theta}{1+\theta/\beta}\right) \approx \exp(\theta)$. Consequently, the Jacobian matrix of the approximated source term from Eq.(5) can be written as:

$$J(\theta, c_F) = \begin{pmatrix} -1 + B\ Da\ (1 - c_F)e^{\theta} & -B\ Da\ e^{\theta} \\ Da\ (1 - c_F)e^{\theta} & -1 - Da\ e^{\theta} \end{pmatrix}. \tag{8}$$

Inserting the steady-state solution Eq.(7) into the $J(\theta, c_F)$, we obtain:

$$J(\theta^{\text{ss}}) = \begin{pmatrix} -1 + B\ Da\ (1 - \frac{\theta^{\text{ss}}}{B})e^{\theta^{\text{ss}}} & -B\ Da\ e^{\theta^{\text{ss}}} \\ Da\ (1 - \frac{\theta^{\text{ss}}}{B})e^{\theta^{\text{ss}}} & -1 - Da\ e^{\theta^{\text{ss}}} \end{pmatrix}, \tag{9}$$

and the corresponding two eigenvalues of the considered dynamical systems are:

$$\lambda_1 = -1.0, \quad \lambda_2(\theta^{\text{ss}}) = -1 + (B - 1 - \theta^{\text{ss}})Da\ e^{\theta^{\text{ss}}}. \tag{10}$$

Both eigenvalues are real, and at least one eigenvalue is a negative constant ($\lambda_1 = -1.0$), which is independent of the steady-state solutions and model parameters. The stability of the system depends on the sign of the second eigenvalue (λ_2). If $\lambda_2 < 0$, the steady-state along the manifold is asymptotically stable, meaning perturbations will decay over time [20,21]. However, if $\lambda_2 > 0$, the steady-state becomes unstable and behaves like a saddle point [20,21]. To investigate how the sign of λ_2 varies with respect to θ^{ss}, we first identify the zeros of λ_2 for the regime $\theta^{\text{ss}} > 0$. Two such zeros are obtained, namely:

$$\theta_1^{\text{ss}} = \theta_{\text{Ext}}^{\text{ss}} = B - 1 + \text{W}_{-1}\left(-\frac{e^{1-B}}{Da}\right),$$
$$\text{and } \theta_2^{\text{ss}} = \theta_{\text{Ign}}^{\text{ss}} = B - 1 + \text{W}_0\left(-\frac{e^{1-B}}{Da}\right), \tag{11}$$

in which W_0 and W_{-1} are two branches of Lambert W function [22]. By obtaining these two zeros, we can determine the corresponding sign of λ_2 depending on θ^{ss} in each interval analytically as

$$\lambda_2(\theta^{\text{ss}}) < 0\text{: } \mathbf{I}_1 = \left\{\theta^{\text{ss}} : 0 < \theta^{\text{ss}} < \theta_{\text{Ext}}^{\text{ss}}\right\} \text{ or}$$
$$\mathbf{I}_2 = \left\{\theta^{\text{ss}} : \theta^{\text{ss}} > \theta_{\text{Ign}}^{\text{ss}}\right\},$$
$$\lambda_2(\theta^{\text{ss}}) > 0\text{: } \mathbf{I}_3 = \left\{\theta^{\text{ss}} : \theta_{\text{Ext}}^{\text{ss}} < \theta^{\text{ss}} < \theta_{\text{Ign}}^{\text{ss}}\right\}.$$

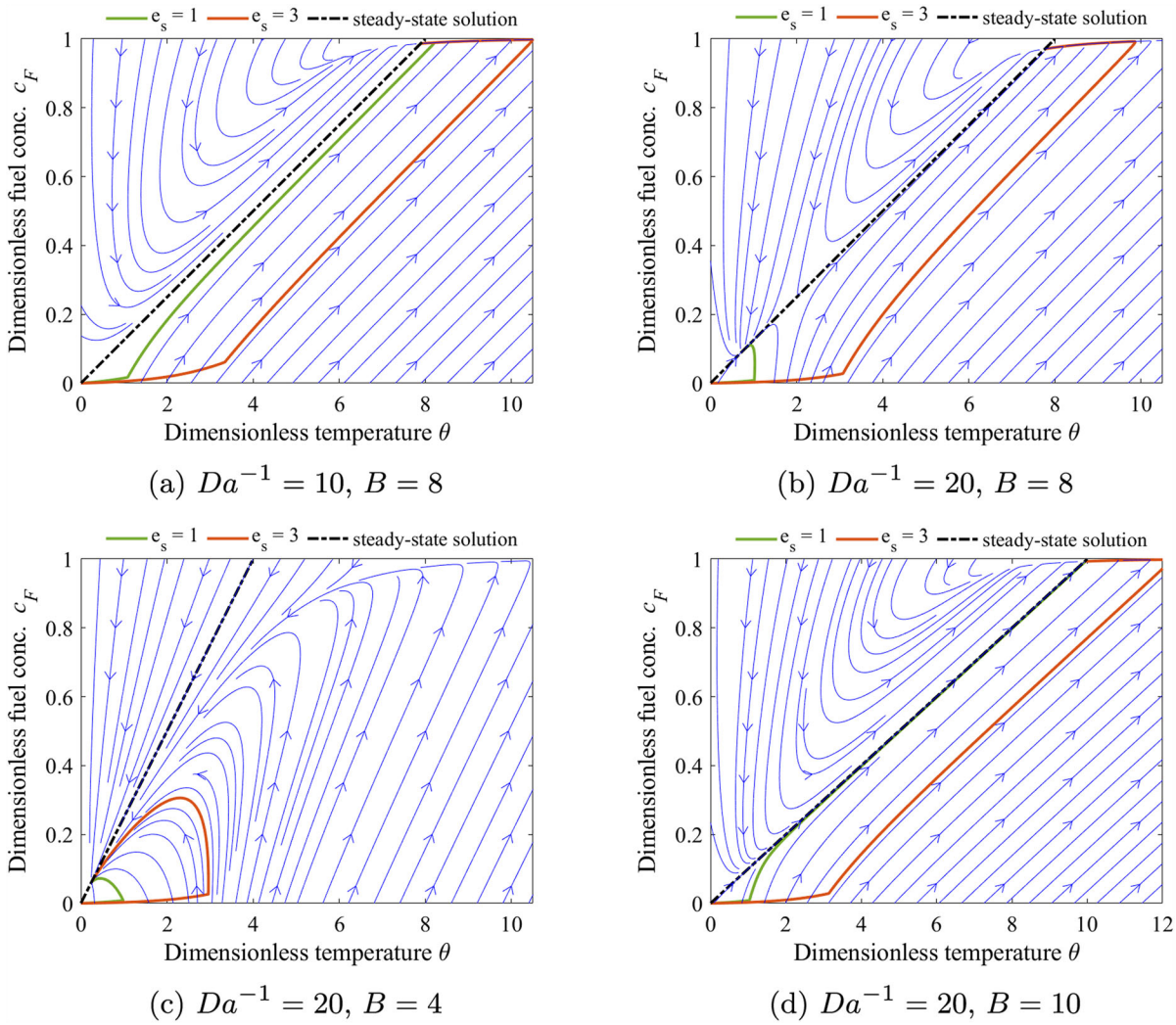

Fig. 3 Phase portraits in c_F-θ phase space for $\tau_s = 0.1$, $\beta = 40$. Green lines: $e_s = 1.0$; Red lines: $e_s = 3.0$.

This analytical solution for the second eigenvalue $\lambda_2(\theta^{ss})$ shows several important aspects:

- There are two regimes, denoted as $\mathbf{I}_1$ and $\mathbf{I}_2$, where stable steady-state solutions are obtained. If θ^{ss} falls within $\mathbf{I}_1$, the system reaches a stable regime corresponding to a failed spark ignition solution. If θ^{ss} falls within $\mathbf{I}_2$, the system reaches the other stable regime where successful spark ignition is achieved.
- The stable regimes ($\mathbf{I}_1$ and $\mathbf{I}_2$) are highly dependent on the model parameters, particularly the dimensionless heat release B and the Damköhler number Da. This dependence also explains the different phase portraits shown in Fig. 3 for two different Damköhler numbers.

Figure 4 shows dependence of θ^{ss}_{Ext} and θ^{ss}_{Ign} on dimensionless heat release B (left) and on Damköhler number (right). The left subfigure in Fig. 4 indicates that θ^{ss}_{Ign} changes only slightly with the Damköhler number, while θ^{ss}_{Ext} increases with Da^{-1} values. This means that with a smaller Damköhler number (larger Da^{-1} value, shorter residence time or longer chemical reaction time-scale), the stable $\mathbf{I}_1$ regime becomes wider, and the system is more likely to encounter a failed ignition solution.

The right subfigure in Fig. 4 shows an interesting phenomenon. At small values of dimensionless heat release (in this figure, when B is less than approximately 5.0), the unstable regime $\mathbf{I}_3$ does not exist.

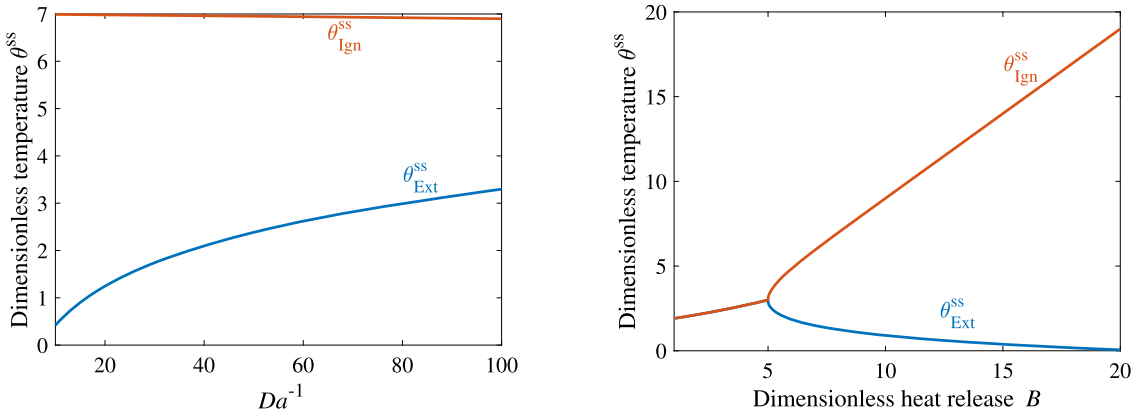

(a) $B = 8$ (b) $Da^{-1} = 20$.

Fig. 4 Dependence of θ^{ss}_{Ext} and θ^{ss}_{Ign} on dimensionless heat release B (left) and on Damköhler number (right). Other dimensionless variables are $\tau_s = 0.1$, $\beta = 40$

As the B-value increases, the unstable regime widens. Even more noticeable, for large values of B, the stable extinction regime $\mathbf{I}_1$ narrows, with θ^{ss}_{Ext} approaching zero. Physically, this indicates that with very high reaction heat release, the system is far less likely to experience failed spark ignition and is more likely to being successfully ignited.

4 Results and discussion

In this part, we will focus on the physical reasons behind these behaviors. The ODE system in Eq.(5) will be numerically integrated directly. Three key dimensionless variables – Damköhler number (Da), spark duration time (τ_s), and the dimensionless heat release (B) – will be varied, and their impact on the ignition process will be discussed in detail. By analyzing these parameters, we aim to gain deeper insights into how they influence the transition between successful and failed ignition states.

4.1 Effect of damköhler number Da

Figure 5 shows the dimensionless fuel conversion in steady state (c^{ss}_F) plotted against the inverse of the Damköhler number (Da^{-1}), for different dimensionless spark ignition energies (e_s). The upper curves represent successful spark ignition, while the lower curves represent spark ignition failure. For each specific e_s, there exists a critical Damköhler number (Da_c), such that no successful spark ignition can be achieved for all $Da < Da_c$ (or $Da^{-1} > Da_c^{-1}$).

First of all, it is interesting to observe that no spark ignition energy is required (as shown by the blue line for $e_s = 0$) when the Damköhler number (Da) is sufficiently large. This occurs because, in such cases, the chemical reaction rate is significantly faster than the convective mass transport rate, allowing the gas mixture to self-ignite. This self-ignition can be achieved when the gas mixture has a sufficiently high initial temperature, resulting in a shorter ignition delay time.

As the spark ignition energy is introduced into the system, the curve in Fig.5 shifts towards larger values of Da^{-1} (indicating shorter τ_R or longer τ_{chem}). This is expected, as the deposition of spark energy heats the gas mixture, significantly increasing the corresponding chemical reaction rate after spark ignition. Therefore, if the residence time τ_R becomes shorter (or a higher convective mass transport rate), the added spark energy helps to accelerate the chemical reactions, enabling the system to achieve successful ignition.

From this figure it is also confirmed that, for each Damköhler number, there exists a minimum e_s, commonly referred to as the dimensionless minimum ignition energy (e^{min}_s), such that the gas mixture can be successfully ignited using a spark. This minimum energy represents the critical threshold required to initiate a successful ignition in the gas mixture. If the applied

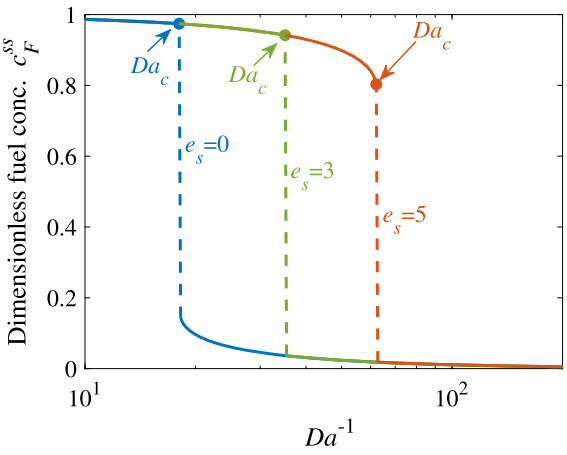

Fig. 5 dimensionless fuel conversion in steady state c_F^{ss} versus the inverse of Damköhler number (Da^{-1}) with dimensionless variables $B = 8$, $t_s = 0.1$, $\beta = 40$

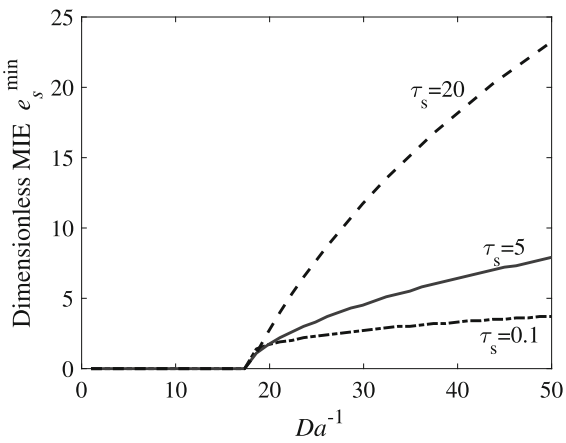

Fig. 6 Dimensionless minimum ignition energy ($e_s^{\min}$) versus inverse of Damköhler number (Da^{-1}) for three different dimensionless spark duration time τ_s with dimensionless variables $B = 8$, $\beta = 40$

ignition energy is below this threshold, the spark will fail to ignite the mixture, whereas exceeding this minimum ensures that combustion can be initiated effectively. To illustrate this, Fig. 6 presents the dimensionless minimum ignition energy ($e_s^{\min}$) plotted against the inverse of the Damköhler number (Da^{-1}) for three different dimensionless spark duration times (τ_s).

It is clearly observed that for a given τ_s, systems with smaller Damköhler numbers (or larger Da^{-1}) require a higher minimum spark ignition energy, $e_s^{\min}$, to achieve successful ignition. This can be attributed to two key reasons: Firstly, for flows with smaller Da-values (indicating a higher convective mass transport rate), a larger amount of the gas mixture passes through the reactor and needs to be heated. Consequently, more spark ignition energy is required to raise the temperature of the gas mixture sufficiently for ignition. Secondly, when more spark ignition energy is provided, the gas mixture is heated to a higher temperature. This leads to an increase in the chemical reaction rate, allowing it to overcome the high convective mass transport rate characteristic of flows with smaller Da-values. As a result, the gas mixture can be successfully ignited by the spark.

4.2 Effect of spark duration time τ_s

In this section, the effect of spark duration time τ_s on the minimum ignition energy (MIE) is examined. Figure 7 shows the dimensionless minimum ignition energy ($e_s^{\min}$) plotted against the dimensionless spark duration time (τ_s) for three different Damköhler numbers.

It is observed that for each Damköhler number, the minimum ignition energy (MIE) $e_s^{\min}$ changes only slightly for short spark duration times but increases rapidly as the spark duration time becomes longer. A closer look indicates that the 'almost' invariance of $e_s^{\min}$ with respect to the dimensionless spark duration time τ_s occurs when $\tau_s < 10^0$, indicating the regime where the spark duration time is shorter than the residence time ($\widetilde{\tau}_s < \widetilde{\tau}_R$). Under this condition, the entire spark ignition energy is deposited into the gas mixture before it leaves the reactor, so $e_s^{\min}$ remains nearly unchanged for $\tau_s < 10^0$.

However, as the spark duration time increases, some of the spark energy heats the gas mixture that exits the reactor due to the short residence time. Fresh cold gas then enters the reactor, reducing the overall temperature of the mixture inside. Consequently, additional spark energy is required to heat both the mixture still inside the reactor and the fresh gas entering. The longer the spark duration time, the more fresh gas enters the reactor, further cooling the mixture, and thus, more spark energy is required to maintain ignition.

4.3 Effect of dimensionless heat release B

The dimensionless heat release provides a measure of the energy released during the combustion of the gas mixture. Most combustion processes involve exother-

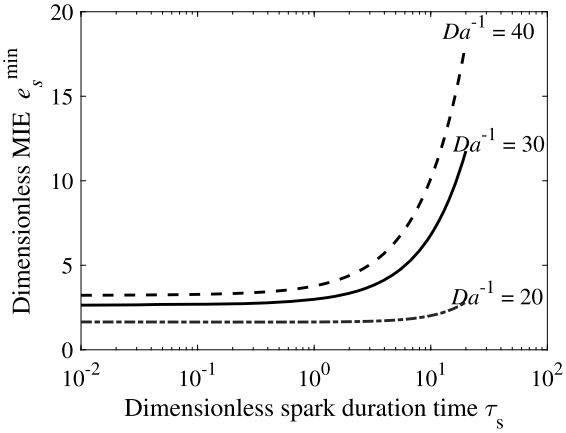

Fig. 7 Dimensionless minimum ignition energy ($e_s^{\min}$) versus dimensionless spark duration time (τ_s) for three different Damköhler numbers with dimensionless variables $B = 8$, $\beta = 40$

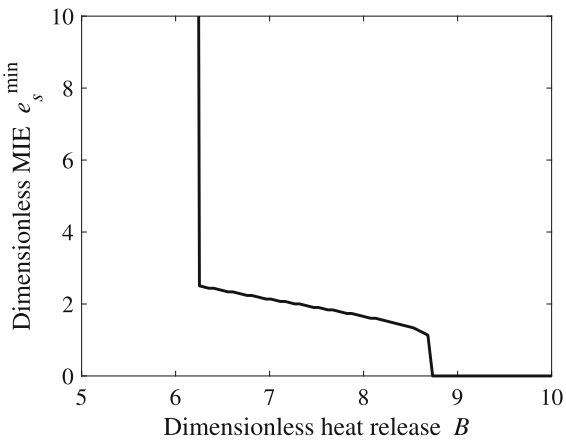

Fig. 8 Dimensionless minimum ignition energy ($e_s^{\min}$) versus dimensionless heat release (B) with dimensionless variables $\tau_s = 0.1$, $\beta = 40$ and $Da^{-1} = 20$

mic reactions with significant heat release. According to [23], the heat released during combustion can vary significantly depending on the fuel type. For instance, the heat released during hydrogen combustion is approximately three times greater than that during methane combustion. Therefore, in Fig. 8, the dimensionless minimum ignition energy ($e_s^{\min}$) is plotted against the dimensionless heat release (B).

It is clearly observed that at low heat release (weak exothermic reactions), significantly higher spark energy is required to ignite the system, while the MIE decreases as the heat release increases. This is because, as the reaction becomes more exothermic, more energy is released during combustion, which helps the chemical reaction without the need for as much external energy. At sufficiently high heat release, the energy generated by the reaction itself can fully support the combustion process, maintaining the reaction without additional input. In extreme cases, when the heat release is very high, no spark ignition energy is required at all ($e_s^{\min} = 0$), leading to the possibility of auto-ignition, where the system ignites spontaneously.

5 Conclusions

The classic Perfectly Stirred Reactor (PSR) model is extended by introducing an additional energy source to simulate the spark ignition process in a laminar premixed flame in a counterflow configuration. A non-dimensional governing ODE system is formulated for both temperature and fuel mass fraction, which depends on three key dimensionless variables: dimensionless heat release, dimensionless activation energy, and the Damköhler number.

The ODE system is first analyzed mathematically. Based on the eigenvalue analysis, it is found that the equilibrium steady states exhibit two stable regimes: one corresponding to failed ignition, and the other to successful ignition. Additionally, the failed ignition regime becomes wider as the Damköhler number decreases and narrower with higher heat release from the chemical reaction.

The analysis is then extended by directly integrating the non-dimensional ODE system, exploring the impact of the Damköhler number, spark duration time, and dimensionless heat release on the ignition process and the minimum ignition energy (MIE). The main observations can be summarized as follows:

- When the Damköhler number is sufficiently large, the chemical reaction occurs so rapidly that auto-ignition can be achieved without the need for external spark ignition energy. However, as the Damköhler number decreases (indicating a slower chemical reaction), more spark ignition energy is required.
- The MIE changes slightly for short spark duration times, but increases rapidly as the spark duration time becomes longer.
- The MIE decreases monotonically with increasing heat release from the chemical reaction. If the heat release is sufficiently high, the reaction becomes

strongly exothermic, releasing enough energy during combustion. In such cases, no external spark ignition energy is required.

While the present model focuses on gas-phase combustion, its framework may be extended to two-phase systems by incorporating droplet evaporation effects, for instance through an additional heat of evaporation in the energy equation. This would enable modeling of liquid-fuel ignition processes and is considered a promising direction for future work.

Author contributions C.Yu: conceptualization, methodology, data analysis, visualization, investigation, writing—original draft. F.Minuzzi: methodology, data analysis, validation, writing—review and editing. All authors reviewed the manuscript.

Funding Open Access funding enabled and organized by Projekt DEAL. C.Yu gratefully acknowledges the financial contribution from the Deutsche Forschungsgemeinschaft (DFG) under the project MA 1205/32-1, project number 528274426.

Data availability No datasets were generated or analysed during the current study.

Declarations

Conflict of interest The authors declare that they have no conflict of interest.

References

1. Frendi, A., Sibulkin, M.: Dependence of minimum ignition energy on ignition parameters. Combust. Sci. Technol. **73**(1–3), 395–413 (1990)
2. Maas, U., Warnatz, J.: Ignition processes in hydrogen oxygen mixtures. Combust. Flame **74**(1), 53–69 (1988)
3. Fernández-Tarrazo, E., Gómez-Miguel, R., Sánchez-Sanz, M.: Minimum ignition energy of hydrogen-ammonia blends in air. Fuel **337**, 127128 (2023)
4. Chen, Z., Burke, M.P., Ju, Y.: On the critical flame radius and minimum ignition energy for spherical flame initiation. Proc. Combust. Inst. **33**(1), 1219–1226 (2011)
5. Yu, D., Yue, L., Chen, Z.: Theoretical analysis on the forced ignition of a quiescent mixture by heat and radical sources. Proc. Combust. Inst. **40**(1–4), 105549 (2024)
6. Yu, D., Chen, Z.: Premixed flame ignition: Theoretical development. Prog. Energy Combust. Sci. **104**, 101174 (2024)
7. Yu, C., Eckart, S., Essmann, S., Markus, D., Valera-Medina, A., Schießl, R., Shu, B., Krause, H., Maas, U.: Investigation of spark ignition processes of laminar strained premixed stoichiometric nh3-h2-air flames. J. Loss Prev. Process Ind. **83**, 105043 (2023)
8. Yu, C., Markus, D., Schießl, R., Maas, U.: Numerical study on spark ignition of laminar lean premixed methane-air flames in counterflow configuration. Combust. Sci. Technol. **195**(9), 2085–2109 (2023)
9. Jenkins, K., Klein, M., Chakraborty, N., Cant, R.: Effects of strain rate and curvature on the propagation of a spherical flame kernel in the thin-reaction-zones regime. Combust. Flame **145**(1–2), 415–434 (2006)
10. Eichenberger, D., Roberts, W.: Effect of unsteady stretch on spark-ignited flame kernel survival. Combust. Flame **118**(3), 469–478 (1999)
11. Brad, R., Tomlin, A., Fairweather, M., Griffiths, J.: The application of chemical reduction methods to a combustion system exhibiting complex dynamics. Proc. Combust. Inst. **31**(1), 455–463 (2007)
12. Shan, R., Lu, T.: A bifurcation analysis for limit flame phenomena of dme/air in perfectly stirred reactors. Combust. Flame **161**(7), 1716–1723 (2014)
13. Wei, J., An, J., Wang, N., Zhang, J., Ren, Z.: Velocity nonuniformity and wall heat loss coupling effect on supersonic mixing layer flames. Aerosp. Sci. Technol. **141**, 108545 (2023)
14. Buckmaster, J., Mikolaitis, D.: The premixed flame in a counterflow. Combust. Flame **47**, 191–204 (1982)
15. Sung, C., Liu, J., Law, C.: On the scalar structure of nonequidiffusive premixed flames in counterflow. Combust. Flame **106**(1–2), 168–183 (1996)
16. Turns, S.R.: Introduction to Combustion, vol. 287. McGraw-Hill Companies, New York, NY, USA (1996)
17. Ma, W., Wang, Q., Dai, L., Yu, C.: Minimum ignition energy density of premixed nh3–h2 counterflow flames. Energy & Fuels (2025)
18. Buckmaster, J.D.: The Mathematics of Combustion. SIAM, Philadelphia, USA (1985)
19. Zeldovich, I.: Mathematical theory of combustion and explosions. Consultants Bureau (1985)
20. Bhatia, N.P., Szegö, G.P.: Dynamical Systems: Stability Theory and Applications. Springer, Berlin, Heidelberg (2006)
21. Leipholz, H.: Stability Theory: An Introduction to the Stability of Dynamic Systems and Rigid Bodies. Springer, Wiesbaden (2013)
22. Lehtonen, J.: The lambert w function in ecological and evolutionary models. Methods Ecol. Evol. **7**(9), 1110–1118 (2016)
23. Linstrom, P.: Nist standard reference database number 69. nist office of data and informatics. NIST Chemistry WebBook. (2021) https://doi.org/10.18434/T4D303